The Impact of Dimensionality on Long-Term Cloud-Resolving Model Simulations

A. M. TOMPKINS

Max-Planck-Institut für Meteorologie, Hamburg, Germany

ABSTRACT

Cloud-resolving model simulations of radiative–convective equilibrium are conducted in both two and three dimensions (2D and 3D) to examine the effect of dimensionality on the equilibrium statistics. Convection is forced by a fixed imposed profile of radiative cooling and surface fluxes from fixed temperature ocean.

In the control experiment, using the same number of grid points in both 2D and 3D and a zero mean wind, the temperature and moisture profiles diverge considerably after a few days of simulations. Two mechanisms are shown to be responsible for this. First, 2D geometry causes higher perturbation surface winds resulting from deep convective downdrafts, which lead to a warmer, moister boundary layer and a warmer tropospheric mean temperature state. Additionally, 2D geometry encourages spontaneous large-scale organization, in which areas far away from convection become very dry and thus inhibit further convection there, leading to a drier mean atmosphere.

Further experiments were conducted in which horizontal mean winds were applied, adopting both constant and sheared vertical profiles. With mean surface winds that are of the same magnitude as downdraft outflow velocities or greater, convection can no longer increase mean surface fluxes, and the temperature differences between 2D and 3D are greatly reduced. However, the organization of convection still exists with imposed wind profiles. Repeating the experiments on a small 2D domain produced similar equilibrium profiles to the 3D investigations, since the limited domain artificially reduces surface wind speeds, and also restricts mesoscale organization.

The main conclusions are that for modeling convection that is highly two-dimensionally organized, such as squall lines or Walker-type circulations over strong SST gradients, and for which a reasonable mean surface wind exists, it is possible that a 2D model can be used. However, for random or clustered convection, and especially in low wind environments, it is highly preferable to use a 3D cloud model.

1. Introduction

In recent years, the number of situations to which cloud-resolving models (CRMs) have been applied has increased substantially. Originally used mainly to investigate individual convective systems (e.g., Schlesinger 1973; Schlesinger 1978), they have more recently been applied to testing assumptions of convective-parameterization schemes (e.g., Xu and Arakawa 1992), investigating the statistics of convection (e.g., Robe and Emanuel 1996), and the modeling of larger-scale convective systems (e.g., Dharssi et al. 1997; Grabowski et al. 1996b) to name just a few examples.

Additionally, a recent series of studies have integrated the CRM for long periods of several weeks in order to investigate radiative–convective equilibrium in the Tropics (Held et al. 1993; Sui et al. 1994; Lau et al. 1993; Grabowski et al. 1996a). These studies have a feature in common in that, like many earlier CRM in-

vestigations, they all adopted a 2D rather than 3D model, often justifying this choice by the assertion that 2D models are computationally more economical, permitting longer integration times. Tompkins and Craig (1998a) and Tompkins and Craig (1999) chose instead to adopt a 3D cloud model for their equilibrium state investigations. A number of other studies have also used 3D CRMs in long-term simulations (e.g., Islam et al. 1993; Robe and Emanuel 1996; Grabowski et al. 1998).

Considering the wealth of both 2D and 3D CRM investigations that have been conducted, a natural question that arises is whether a 2D cloud model reproduces similar cloud statistics to a 3D model. Bretherton and Smolarkiewicz (1989) examined the nature of subsidence associated with a heat source in 2D and 3D geometry using a linear model, and it was shown that 2D geometry artificially spreads this subsidence. Thus one would perhaps expect that limiting cloud-scale motions to two dimensions would alter characteristics of convection, such as the transport of water vapor to the upper troposphere, with the possible exception of specifically two-dimensional convective structures such as squall lines (although, of course, these systems must still possess non-slab-symmetric cloud draft structure).

Corresponding author address: A. M. Tompkins, Max-Planck-Institut für Meteorologie, Bundesstrasse 55, D-20146 Hamburg, Germany.
E-mail: Tompkins@dkrz.de

Some previous numerical studies have compared 2D and 3D CRMs (Tao and Soong 1986; Tao et al. 1987) and reported that many convective statistics such as precipitation were very similar, although they observed stronger downdrafts in the 2D experiments and also differing momentum transport properties. There could be many reasons for the similarities. The convection in these experiments was subjected to large-scale wind shear, which organized the convection into banded 2D structures, which would maybe reduce the contrast between 2D and 3D simulations. Another reason could simply be that the experiments were short term, modeling only the transient response of convection. The arguments made by Emanuel (1994) concerning the testing of cumulus parameterization schemes apply equally well to the test of dimensionality. The difference in convective heating and moistening profiles comparing 2D and 3D simulations may only appear to be a small fraction of the instantaneous rates, but may in fact represent a significant trend that would result in very different equilibrium states over a longer period of time. A recent study of Grabowski et al. (1998) did perform a longer period integration and also reported little sensitivity to dimensionality, in terms of quantities such as relative humidity, stating that the main differences were that the 2D investigations exhibited much higher temporal variability, although it will be shown in the following section that most of the difference in variability was probably due to the smaller number of horizontal grid points used in the 2D simulations.

To investigate this issue further, we examine the differences in radiative–convective equilibrium statistics that occur in between two and three dimensions using a CRM. The following section describes the model and the setup for the experiments based on some preliminary investigations. Section 3 then describes the control comparison, with mechanisms for the differences discovered proposed in section 4. Further experiments conducted in section 5 investigate the generality of the findings.

2. Model and setup

a. Model

A detailed description of the CRM is contained in Shutts and Gray (1994). The basic cloud model is anelastic with an advanced total variation diminishing scheme for advection of all prognostic quantities (Leonard 1991). The microphysical scheme integrates prognostic equations for rain, snow, cloud water, cloud ice, and graupel amounts (Brown and Swann 1997). In the microphysical scheme only the categories of snow, graupel, and rain are assumed to have nonzero fallspeeds. The surface fluxes are provided using similarity theory that obviates the requirement for a minimum surface wind speed necessary if a bulk aerodynamic formula is used. Since the investigation is concerned with identifying sensitivities specifically due to dimensionality,
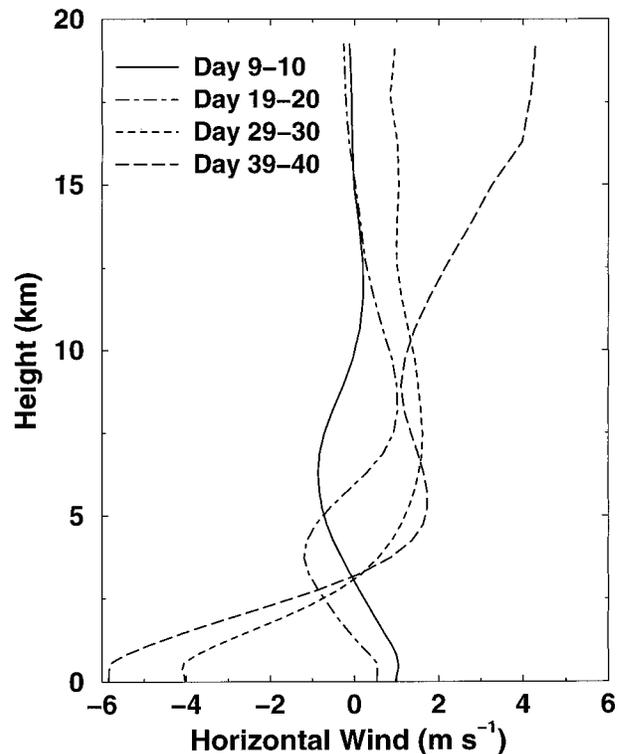

Fig. 1. One-day average model mean horizontal wind as a function of height at 10-day intervals throughout the 2D preliminary investigation with unconstrained mean winds.

fixed radiative forcing was used to prevent radiative–convective feedbacks. In the preliminary experiments the cooling profile was taken from the equilibrium state of Tompkins and Craig (1998a).

b. Preliminary investigations with unconstrained winds

A preliminary investigation was conducted using the 31-level vertical grid of Tompkins and Craig (1998a), and 900 horizontal grid points (arranged as a 30 × 30 grid in the 3D case), with the integrations lasting 40 days. It was found that during the course of the experiments a vertical wind shear developed, that remained very weak in the 3D case (less than 1 m s^{-1} across the entire troposphere), but was significant in the 2D simulation (Fig. 1). This seems to be a commonly occurring feature of 2D CRMs that do not use constrained winds and was seen in previous simulations by Held et al. (1993) and Wyant et al. (1997), for example. Note that many of the other long-term simulation investigations cited in the introduction constrained the vertical wind to a given mean profile and thus would not reveal this sort of behavior. The equilibrium state statistics of such quantities as cloud cover and temperature profile differed considerably, as one would expect, since the wind shear acts to organize convection and can greatly alter

the balance between updrafts and downdrafts (Cheng 1989). However, the feedback of the wind shear is undesirable since it may obscure differences that occur due to the dimensionality of the simulations themselves. Thus it was decided to remove the wind shear by constraining the horizontal winds. This was done by introducing an artificial momentum source as

$$\frac{\partial V}{\partial t} = \frac{V_t - \overline{V}}{\Delta t}, \tag{1}$$

where V is the horizontal wind velocity, with the subscript t and the overbar representing the target velocity and the horizontal mean, respectively, both functions of height, and Δt is the time step of the model. The target velocity is simply set to zero at all heights unless otherwise specified. Other studies often choose to use a longer timescale on the order of hours instead of the model time step to relax the mean velocities (e.g., Grabowski et al. 1996b). However, the slower timescale still allows differences in the mean wind profiles to develop, albeit reduced, and since the effect of wind shear is likely to be highly nonlinear, the slow relaxation timescale cannot be used here. Examination of cloud snapshots reveals that adjusting the mean wind over a single time step did not constrain the cloud-scale circulations in any way, since the momentum source of the developing wind shear is very small in magnitude compared to that associated with cloud-scale motions.

c. Preliminary investigations with constrained winds

Recently Tompkins and Craig (1998a) suggested that in order to simulate a steady radiative–convective equilibrium with continuously active convection, the critical factor (assuming convection is well resolved) is whether a sufficiently large domain is used to represent the subsidence region surrounding a single convective cloud. If the domain is too small, convection will become sporadic, with convective bursts separated by inactive periods during which surface fluxes and radiative cooling restore convective instability. It is not clear that extensive time averaging of statistics of an experiment using a significantly undersized domain will match those of larger domains, since the system treated is far from linear, especially if an interactive radiation scheme is used to provide the forcing for convection. For example, Robe and Emanuel (1996) stated that convective statistics in their 3D equilibrium studies, using a CRM with fixed radiative forcing, appeared independent of the domain size used, but found that the behavior of the domain mean Convective Available Potential Energy was significantly altered (and thus also the mean temperature and vapor profiles) when forcing was reduced to such an extent that the domain size was insufficient and convection became intermittent. Tompkins and Craig (1998a) proposed that the issue of computational cost is independent of dimensionality, suggesting that if a typical radiative forcing of 1 K d^{-1} requires an $O(10^3$

TABLE 1. Preliminary runs.

Dimensions	Number of horizontal grid points
3D—60 km $\times$ 60 km	900
2D—1800 km	900
3D—120 km $\times$ 120 km	2700
2D—120 km	60

km^2) domain to contain the subsidence balancing a continuous convective updraft, then this is true of both two as well as three-dimensional simulations.

To investigate this further, a number of 15-day preliminary runs were conducted, which are summarized in Table 1. First, two runs were performed with an identical number of horizontal grid points (900) arranged in two and three dimensions. A third 3D run was performed with a domain four times larger to show that the domain used is sufficiently large. A fourth 2D run used a short domain of 120 km (the length of one side of the large 3D run), since it is possible that differences between 2D and 3D may occur due to the fact that the long 2D domain could allow mesoscale organization of convection that would be prohibited in the limited 3D domain. All four experiments used the 31-level vertical grid and a 2-km horizontal resolution, with horizontal winds constrained to zero as outlined above.

To examine the intermittency of the convection, Fig. 2 shows time series of the maximum vertical velocity anywhere in the domain for all three cases. If one assumes that a vertical velocity exceeding 1 m s^{-1} indicates the presence of convection (e.g., LeMone and Zipser 1980; Robe and Emanuel 1996), then the graph for the 120-km 2D runs reveals a strong intermittency, with the maximum velocity remaining below the convective threshold for long periods of time. The same level of intermittency was reproduced in a further 120-km 2D experiment that used a very fine horizontal resolution of 133 m (not shown), indicating that it is a result of the highly restricted domain size and not an artifact of the small number of grid points.

Comparing the upper two panels of Fig. 2, which use the same number of grid points, the maximum velocity in both cases always remains above 1 m s^{-1}, but with a large range, indicating that the domains are just above the threshold size required to continuously contain convective activity. In terms of the range and frequency, it is extremely difficult to determine any difference between the two panels at all, proving that the frequency of convection is independent of the dimensionality, as proposed by Tompkins and Craig (1998a). For comparison, the vertical velocity in the 120 km $\times$ 120 km 3D case rarely drops below 10 m s^{-1}, since the domain is sufficient to always have many concurrent cases of deep convection.

The water vapor profile is one of the most difficult quantities to predict by models (Emanuel 1991), and therefore Fig. 3 shows the evolution of the total col-
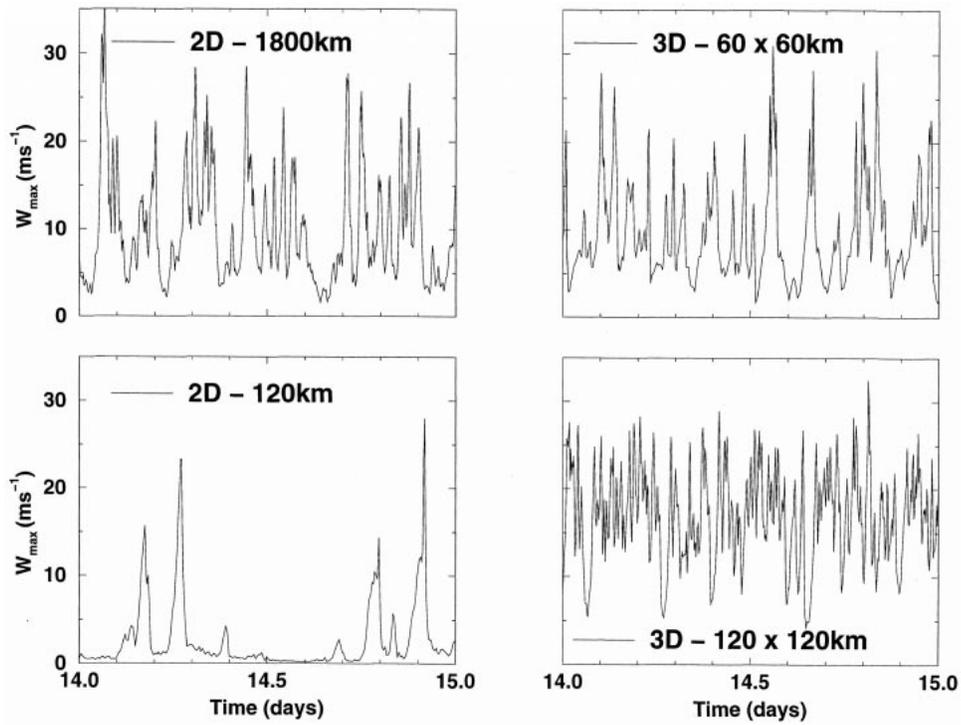
FIG. 2. Time series of maximum vertical velocity within the domain for four preliminary experiments with horizontal mean winds constrained to zero.
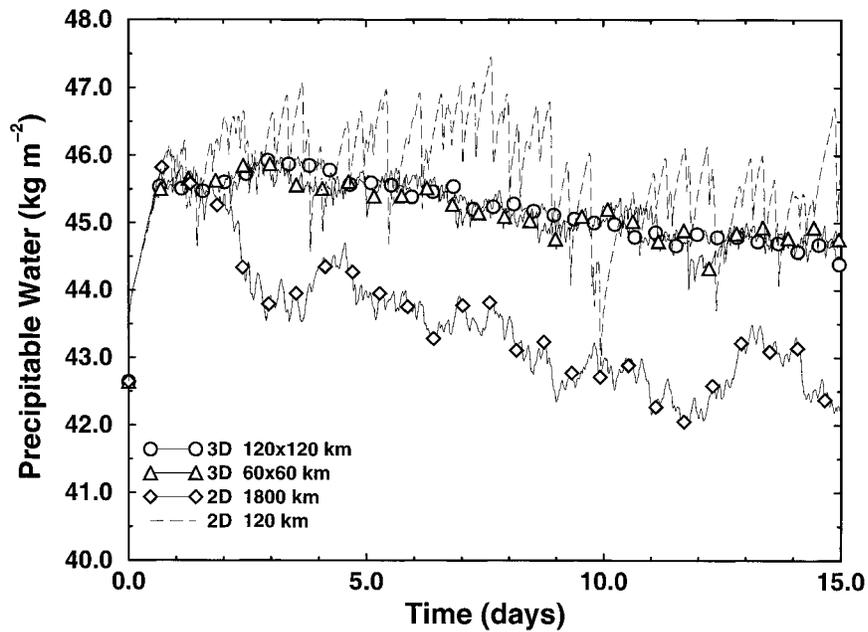

FIG. 3. Time series of total column water vapor for the four preliminary experiments with horizontal mean winds constrained to zero.

TABLE 2. Model setup.

Forcing	2 K day^{-1} until 400 hPa, decreasing to zero at 200 hPa
Number of grid points	30 × 30 × 48 (3D)
	900 × 48 (2D)
	60 × 48 (2D small domain)
Horizontal resolution	2 km
Vertical resolution	Stretched (100–600 m)
Surface fluxes	Monin–Obukhov formulation
Horizontal boundary conditions	Periodic
Upper boundary condition	Fixed lid at 22 km (with sponge layer above 17 km)
Lower boundary condition	Ocean with fixed temperature of 300 K

umn-integrated water vapor. Apart from the fact that the variability is of course greater in the smaller domain, the evolution of water vapor is identical in the two 3D cases, and thus 900 grid points appear to be sufficient for the simulations. The 1800-km 2D domain is much drier in comparison. However, the small 120-km 2D domain renders an atmosphere much more similar to the 3D experiments, although the comparison is made difficult by the large variability on timescales up to several days. This therefore raises the possibility that mesoscale organization of the convection could be present in the 1800-km domain, which is restricted in the smaller domain. This aspect will be investigated further in section 5.

These preliminary investigations lead to the following suggested setup for the main experiments in this paper.

In the control runs, 900 grid points are used in the horizontal, with a resolution of 2 km. The forcing magnitude is increased to 2 K d^{-1} to provide more continuous convection and a faster adjustment timescale (Tompkins and Craig 1998b), simply applied as a constant cooling to 400 hPa, which then decreases linearly to zero at 200 hPa. All experiments are conducted for a period of 20 days, which is just long enough to reach equilibrium at the forcing rate used. Recent results of Tompkins and Emanuel (2000) indicate that an improved vertical resolution to that used in the preliminary experiments is desirable, and thus 48 vertical levels are used, with the resolution slowly stretching from 100 m in the boundary layer to 600 m at 10 km, and is then held constant to the domain lid at 22 km. Each experiment is initialized by a resting cloudless state, with temperature and moisture profiles simply taken from an equilibrium state of a preliminary run. The setup details are summarized in Table 2.

3. Control experiments

a. Approach to equilibrium

In the control experiments, the total column water vapor and atmospheric temperature appear to settle to a quasi steady state by around day 15 (Fig. 4), with both experiments drier than in the preliminary runs, due to the increased magnitude of the forcing. Taking the average over the last 5 days, the 3D simulation has a temperature and total vapor amount of 253.6 K and 41.0
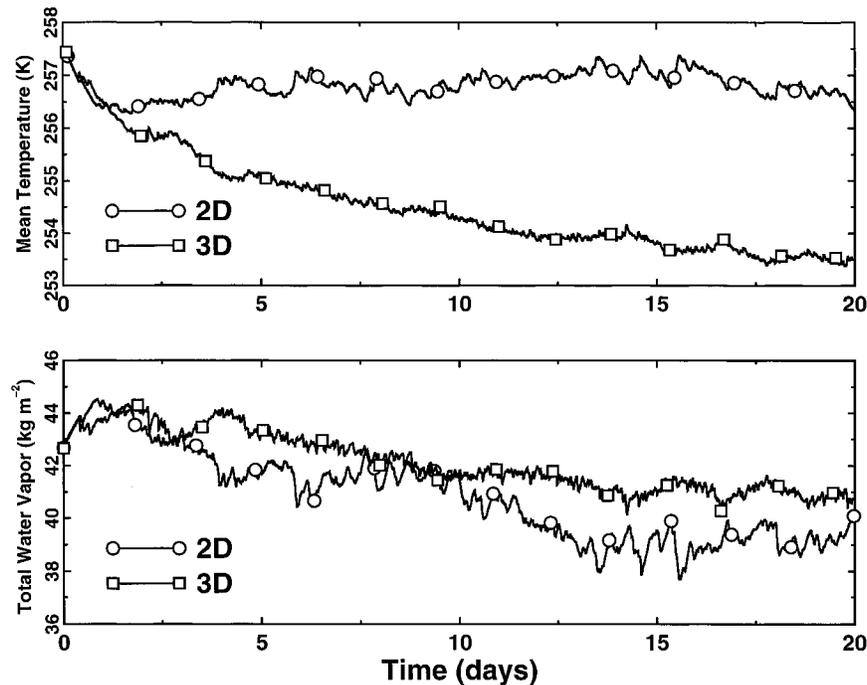

FIG. 4. Time series of mean temperature and total column water vapor for the control run experiments.
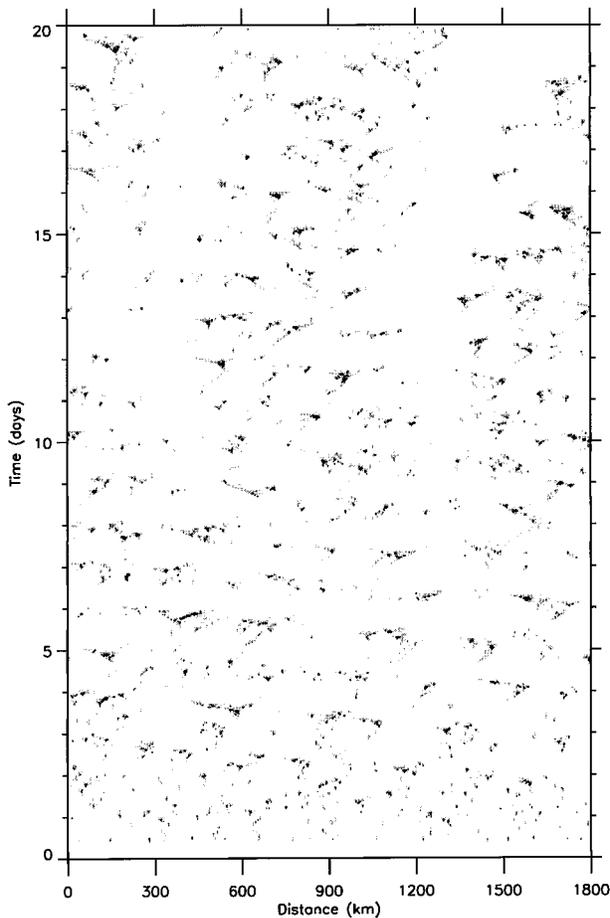
FIG. 5. Hovmöller rainfall plot for the 2D control run. The light and dark shading represent a rain rate of 1 mm h^{-1} and 10 mm h^{-1}, respectively.
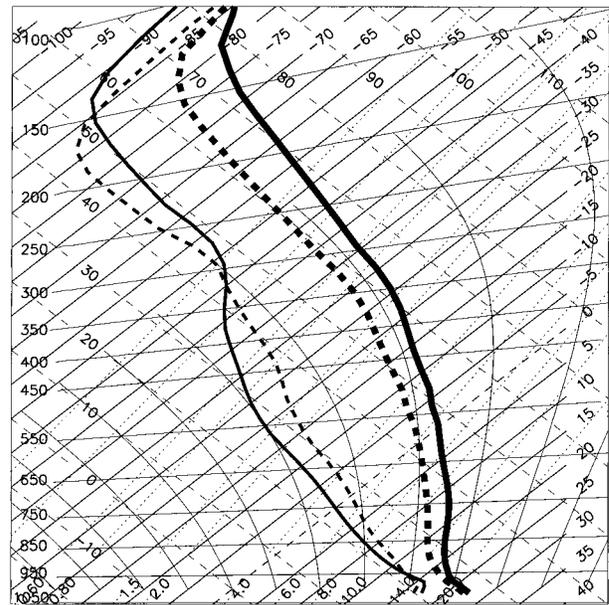

FIG. 6. Tephigram thermodynamic chart plotting the final 5-day average temperature (thick lines) and water vapor (thin lines) for the 2D (solid lines) and 3D (dashed lines) control experiments.

kg m^{-2}, respectively, compared to 256.9 K and 39.2 kg m^{-2} for the 2D case. In can be seen that the differences between the 2D and 3D experiments significantly exceed the temporal variability in both cases. The 2D simulation at times has a higher temporal variability than its 3D counterpart, a possible indication of larger-scale organization of convection.

A Hovmöller diagram of surface rainfall rate in the 2D simulation (Fig. 5) reveals that after a period of 2 or so days of weak scattered convection, the convective activity is more predominately organized into isolated deep convection systems, with relatively short lifetimes of a few hours. Modulation of these systems can be identified. First, careful examination reveals a weak banded structure, in which the systems appear to propagate across the domain at a velocity of around 21 m s^{-1}, consistent with gravity wave propagation. Thus any particular horizontal position experiences convective activity roughly once a day.

A further modulation of convection is apparent in the form of two almost stationary bands almost free of convection, that start to develop between days 8 and 10,

centered at 400 and 1300 km, respectively. The reason for these bands turns out to be an important aspect for the differences between two and three dimensions and is discussed further later.

b. The final state

To examine the vertical structure of the temperature and moisture, Fig. 6 plots the tephigram of the data averaged over the last 5 days. In both cases a well-mixed (in water vapor) boundary layer of constant potential temperature forms, which is both warmer and moister in the 2D case. The temperature structure above the boundary layer closely follows a moist adiabatic, with conditional instability in evidence. The warmer/moister boundary layer of the 2D simulation necessarily leads to the adoption of a warmer adiabat in this case. The moist-adiabatic structure dictates that the greatest temperature differences will occur at the upper troposphere, although in fact the upper-tropospheric differences are approximately 2 K larger than that expected from moist-adiabatic structure alone. On the other hand, the moisture in the 3D run is higher immediately above the boundary layer, and remains so throughout almost all the convecting layer to approximately 300 hPa (9.6 km). The relative humidity is thus significantly higher in 3D from the top of the boundary layer to around 11 km (Fig. 7).

In terms of the other basic convective characteristics, the two cases are fairly similar. For example, examination of the convective mass fluxes (not shown) reveals that the net convective mass flux is slightly greater
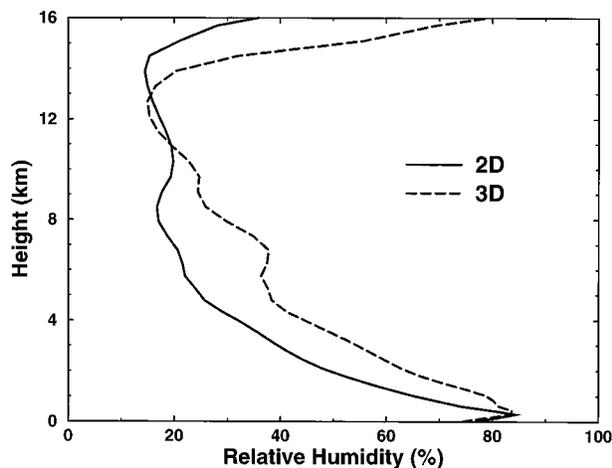
FIG. 7. Final 5-day average relative humidity plotted against height for the control experiments. Above the freezing level the relative humidity is calculated using the ice saturation vapor pressure.
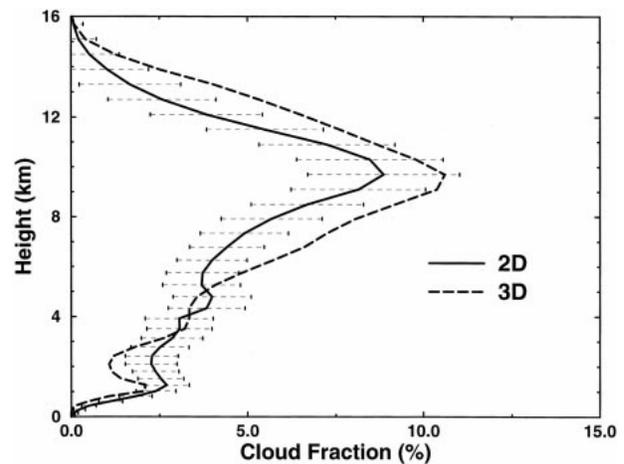

FIG. 8. Final 5-day average cloud fraction plotted against height for the control experiments. The horizontal bars represent ± one standard deviation for the 2D case to represent the variability. For clarity the standard deviations are not shown for the 3D experiment, which are anyway similar to the 2D values.

throughout the troposphere in the 3D. This is to be expected, since the overall convective mass flux is constrained to balance the fixed imposed radiative cooling rate. The cooler moist adiabat adopted in 3D gives slightly smaller potential temperature lapse rates, which in turn would imply a slightly larger mass flux in compensation. The same trend is seen in the total mass flux statistics, but in both cases the trend is small compared to the standard deviation.

The cloud fractions show slightly more significant trends (Fig. 8), with the 3D cloud fraction lower between 900 and 700 hPa and higher between 500 and 100 hPa. The standard deviation is also plotted to give an indication of the cloud fraction temporal variability. To calculate this quantity, a grid point is identified as cloudy if the total condensate mixing ratio exceeds 5×10^{-6} kg kg^{-1} (Sui et al. 1994; Guichard et al. 1997). From all the common methods of calculating cloud fraction this usually produces the lowest estimate, especially in the upper troposphere (Xu and Krueger 1991), but this is not important since only relative differences between 2D and 3D simulations are of interest. Despite the fact that the differences in terms of the ratio of cloud fraction seem significant, with cloud fraction doubling, for example, at the 800-hPa height, the absolute cloud fraction is not changing more than a few percent at any height, and it is unlikely that significant cloud/radiation feedback differences would occur between the two cases if an interactive radiation scheme were used. The total cloud fraction, calculated as the number of columns containing at least one cloudy grid point, is actually slightly larger in the 2D case (20.5% compared to 16.5%), but the difference of 4% is still less than the standard deviation (4.8% and 4.7%, respectively). Out of all the microphysical quantities of rain, liquid cloud, graupel, snow, and ice, only liquid cloud shows a significant trend, with the 3D average column content of

22 g m^{-2} doubling to 44 g m^{-2} in the 2D case, consistent with the doubling of the shallow cloud fraction.

4. Proposed mechanisms

In the control run, it was seen that although the temperature and moisture profiles diverge after a few days of simulation, with the 2D case adopting a significantly warmer and drier state, most other characteristics, such as cloud amounts and mass fluxes do not change significantly. We now attempt to identify mechanisms that can explain these differences.

a. Temperature differences

As noted earlier, the warmer moist adiabatic 2D atmosphere is a direct result of the warmer and more humid boundary layer that develops. Since the mean surface winds are identically zero in both cases, and quasi-equilibrium fluxes of latent and sensible heat are constrained to balance the imposed forcing, one would perhaps assume that the boundary layer water vapor and temperature would also be the same.

The work of Bretherton and Smolarkiewicz (1989) can offer a simple theory to explain why this is not the case. They analyzed the atmospheric response to an idealized point buoyancy source, showing that in 2D, the response involves a constant horizontal velocity everywhere within the adjustment region of the spreading gravity wave packet, which contrasts to the response in 3D, where the outflow velocity decreases with inverse radius. It is easy to imagine the analogous case for the surface outflow from convectively generated downdrafts, which is illustrated schematically in Fig. 9. With three dimensions the downdraft produced from an idealized continuous convective event has to decrease with
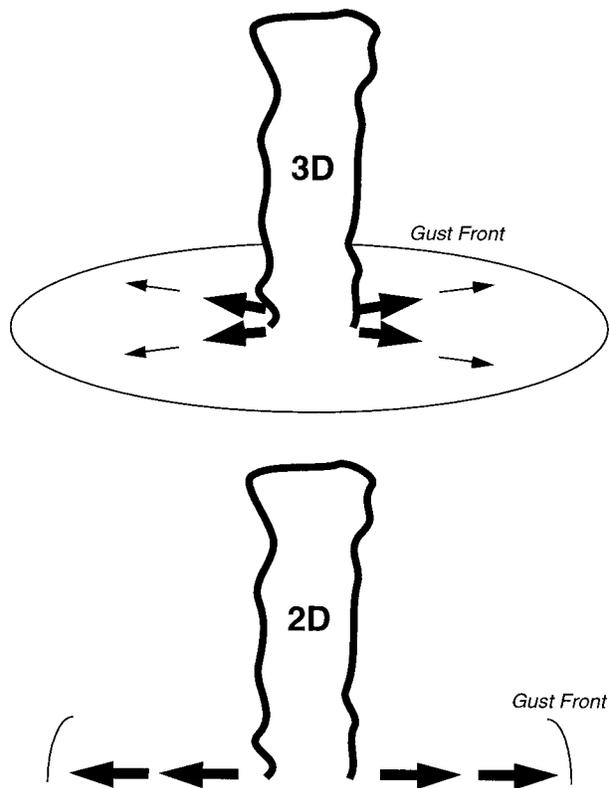
FIG. 9. Schematic of expected differences in surface winds between the case of two and three dimensions. The arrows indicate the surface winds resulting from downdrafts, with thicker arrows representing higher velocities

increasing radius, whereas the artificial restriction of two dimensions requires that the surface winds are maintained at any distance from the convective event that is within the gust front. Thus, although the mean winds are identical in both cases, the perturbation velocity is necessarily higher in 2D.

In a state of radiative–convective equilibrium the total surface fluxes are constrained to balance the imposed radiative cooling rate. Therefore any increase of surface winds must imply a smaller temperature and moisture difference between the boundary layer air and the values imposed at the ocean surface, giving the warmer, more humid boundary layer and associated warmer tropospheric temperatures in 2D. Of course, real convective systems have a limited lifetime, especially in a zero sheared environment where the downdrafts cut off the system (Browning and Ludham 1962; Schlesinger 1973; Schlesinger 1978), and with shorter cumulus lifetimes the 2D–3D contrast could decline. It is straightforward to test this mechanism by examining the mean perturbation surface velocity, $\overline{V'}$, and it is found that the average value for $\overline{V'}$ in 2D of 3.2 m s^{-1} is reduced to 1.7 m s^{-1} when three dimensions are utilized. This implies that the effective surface velocity is approximately twice as large in 2D, and the mean potential temperature dif-

ference between the surface and the lowest model layer is correspondingly reduced from 1.4 to 0.7 K. Although the boundary layer is more moist in 2D, the water vapor mixing ratio difference between 2D and 3D is reduced only by 1.2 g kg^{-1} from 7.2 g kg^{-1} to 6.0 g kg^{-1}, presumably due to the feedback of downdrafts and the drier midtroposphere, thus also implying a different ratio of sensible to latent heat fluxes in the two cases.

b. Water vapor differences

Given the warmer tropospheric temperatures, assuming a constant relative humidity would predict a moister state in 2D, which was seen not to be true. The Hovmöller plot of rainfall in Fig. 5 hinted at a reason for the drier 2D atmosphere, revealing two bands that developed over time, in which convection was almost completely inhibited. The reason for these nonconvective bands is not totally clear. These bands coincide with much lower values of atmospheric water vapor, obvious in instantaneous vapor fields (Fig. 10), which show lateral variations in water vapor exceeding one order of magnitude. Since locally dry atmospheres can greatly inhibit convection due to the reduction of buoyancy when entrained (e.g., Raymond 1995; Mapes and Zuidema 1996; Brown and Zhang 1997; Michaud 1998), this acts as a positive feedback, with convection locally moistening the atmosphere, making further convection there more likely. Concentrating the convection in one part of the domain, reduces the mean vapor content of the atmosphere, since the fraction of convective water rained out as precipitation will be higher if the convection is occurring in a more saturated environment (Anthes 1977). In comparison the lateral variation in water vapor in the 3D experiments is much more limited and convection is observed to propagate throughout the domain. However, it is also possible that the water vapor differences are a result, rather than a cause of the convective organization, and that differences between near-cloud and far-cloud subsidence, such as highlighted by Bretherton and Smolarkiewicz (1989), could also cause the organization of convection on the large scale.

5. Further experiments

a. Nonzero and sheared mean winds

To test the generality of the above mechanisms, two further experiments are conducted. The sensitivity of the perturbation surface winds may be greatly reduced in a situation in which mean surface winds are present. Thus in the first comparison made, a horizontal background mean wind profile is imposed, set to 4 m s^{-1} from the surface to 12 km, reduced linearly above to zero at 15 km. In the second experiment, we attempt to reduce the organization of convection that was possibly caused by the water vapor field. To do this we follow the approach of Held et al. (1993), who applied a mean
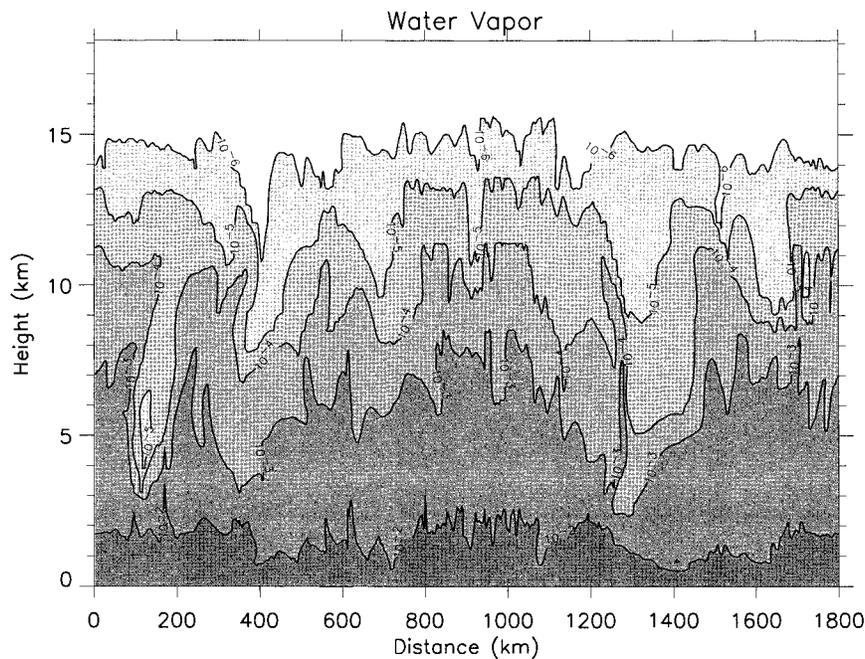
Water Vapor

FIG. 10. Snapshot of the water vapor mass mixing ratio field taken from the end of the 2D control case. The contour values are 10^{-6}, 10^{-5}, 10^{-4}, 10^{-3}, and 10^{-2} kg kg^{-1}.

vertical wind shear to laterally mix water vapor and destroy the localization of convection found in their experiments. The profile used here is similar to that of Grabowski et al. (1996a), and is given in Fig. 11. The two experiments are referred to as the "constant wind" and "sheared wind" cases, respectively, with "zero wind" referring to the control experiment of section 3.

All experiments were conducted for 20 days, and Table 3 gives the mean atmospheric temperature and column water vapor content for the last 5 days of simulation. The higher surface winds of 4 and 8 m s^{-1} in the constant wind and sheared wind cases, respectively,
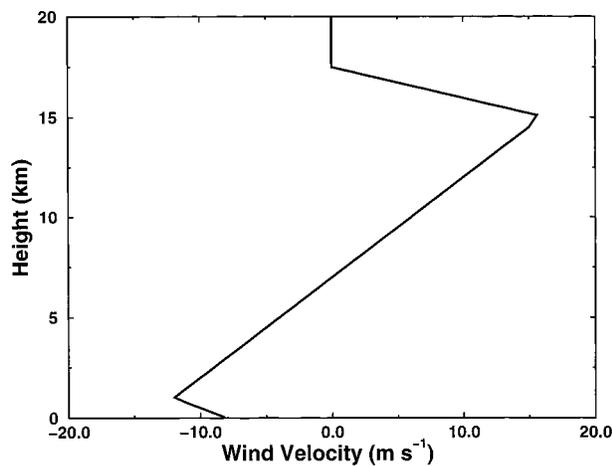

FIG. 11. Imposed mean horizontal wind used in the shear wind experiment.

naturally lead to higher temperatures and water vapor amounts. The temperature difference between 2D and 3D is seen to be smaller for the sheared case (0.6 K) than either the constant wind (1.2 K) or zero wind (3.3 K) cases. On the other hand the difference in total water vapor increases, becoming 4.9 kg m^{-2} in the sheared case.

The Hovmöller diagram for the large 2D constant wind experiment shows similar behavior to the zero wind case, as expected, with short lived convective systems advected at the imposed wind speed (not shown). However, the advection of the systems makes identification of dry bands difficult in a standard Hovmöller plot, and thus Fig. 12 shows the rainfall with a Galilean transform applied. It is quite clear that, again after around 10 days of simulation, two dry bands appear in the domain, which are advected along with the mean wind.

When the mean wind imposed is sheared, the convection becomes organized into long-lived systems that

TABLE 3. Final thermodynamic states.

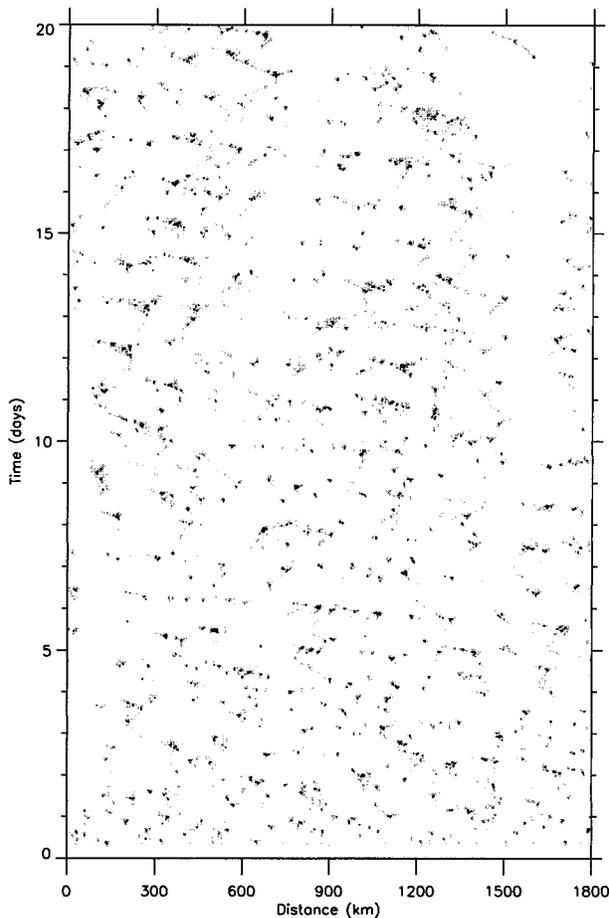| Experiment	Mean temperature (K)	Total water vapor (kg m^{-2})
2D—Zero mean winds	256.9	39.2
3D—Zero mean winds	253.6	41.0
2D—Constant 4 m s^{-1} mean winds	257.9	43.8
3D—Constant 4 m s^{-1} mean winds	256.7	46.0
2D—Sheared mean winds	259.0	51.8
3D—Sheared mean winds	258.4	56.7

FIG. 12. Hovmöller rainfall plot for the 2D constant wind case, with a Galilean transform of -4 m s^{-1} applied to facilitate the identification of convective organization. Contours are identical to Fig. 5.
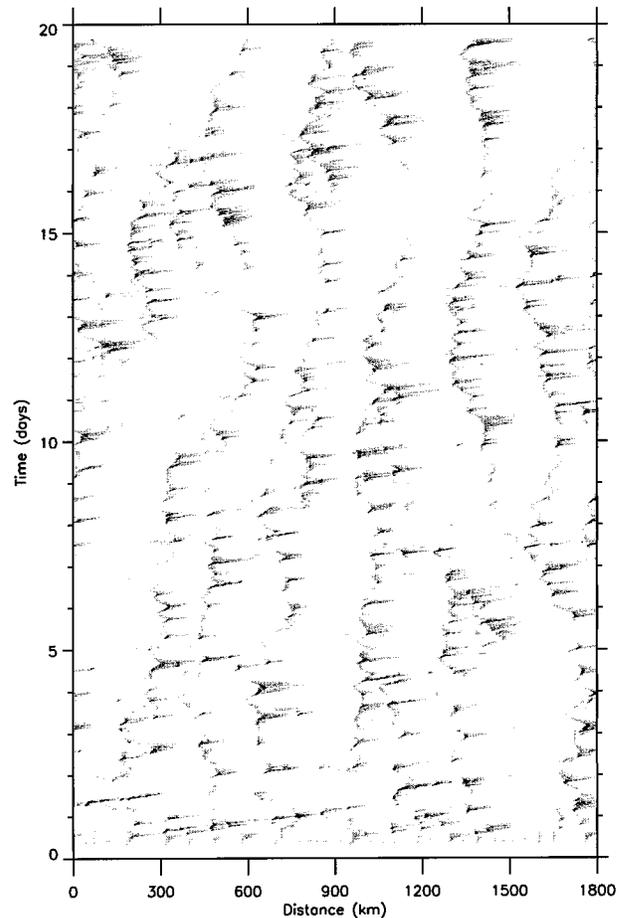

FIG. 13. Hovmöller rainfall plot for the 2D constant wind case, with a Galilean transform of 11 m s^{-1} applied. Contours are identical to Fig. 5.

are advected throughout the domain. Applying a transformation of 11 m s^{-1} (Fig. 13) reveals that the individual propagating systems tend to be organized in groups, indicating that some mesoscale organization still exists in spite of lateral mixing effect of the vertical wind shear. That said, examining the vapor (Fig. 14) reveals it to be more horizontally uniform in the sheared case than the control (Fig. 10).

Figure 15 shows the temperature difference between the 2D and 3D experiments as a function of height, with the corresponding fractional water vapor change given in Fig. 16. The application of a mean surface wind is seen to reduce the temperature and water vapor differences in the lowest model level almost to zero. Thus the differences in perturbation velocity caused by the geometry of two and three dimensions are only significant in situations of low or zero mean surface winds, such that convective downdrafts act to increase mean surface perturbation winds. The similar boundary layer characteristics result in a significant reduction of the temperature differences throughout the troposphere,

with the largest reduction occurring in the sheared case. However, even in the sheared case, upper-atmospheric temperature differences still remain, albeit much reduced, and it is possible that the different mesoscale circulations that derive from the very different organization in 2D and 3D are be the cause of this.

In comparison the trend in the water vapor is less clear, and although the large fractional changes in upper-tropospheric vapor are reduced with an imposed constant or sheared wind, the midtropospheric trend actually increases in the sheared case. This is to be expected though, since first, organization of convection still occurs, and second, the relative moist boundary layer in the 2D control case would have partially offset the drying of organization.

b. Small 2D domain experiments

As mesoscale organization still exists with both constant and sheared background winds, in this section we briefly examine the statistics of three further experiments, which repeated the zero, constant, and sheared
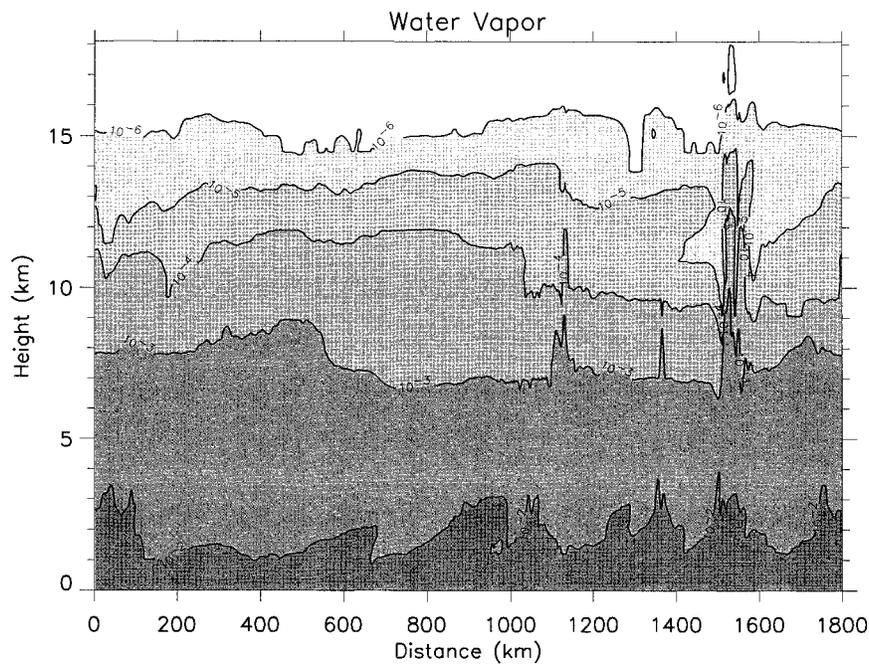
FIG. 14. Snapshot of the water vapor mass mixing ratio field taken from the end of the 2D sheared wind case. The contour values are identical to those in Fig. 10.

wind cases using a small 2D domain of 120 km, with 2-km horizontal resolution.

Table 4 contains the mean atmospheric temperature and column water vapor content for the last 5 days of simulation for comparison with Table 3. In each case the short 2D runs are slightly warmer and wetter than their 3D counterparts, with the values indeed nearer than their 1800-km 2D equivalents runs. The temperature difference and fractional vapor change are shown in Figs. 17 and 18, respectively. They reveal that the temperature and moisture characteristics do not change sig-

nificantly, implying lower surface winds in the small 2D domain than the large one. Examining animations of the convection revealed this to be an artificial restriction, since in 2D, the outflow from downdrafts can cross the 120 km in a few hours, and consequently die out when meeting their "partner" outflow traveling in the opposite direction. (Remember that that this does not occur in the 3D domains, since the geometry ensures that the outflow velocity drops off with distance from the clouds.) Surface winds are then calm for many hours
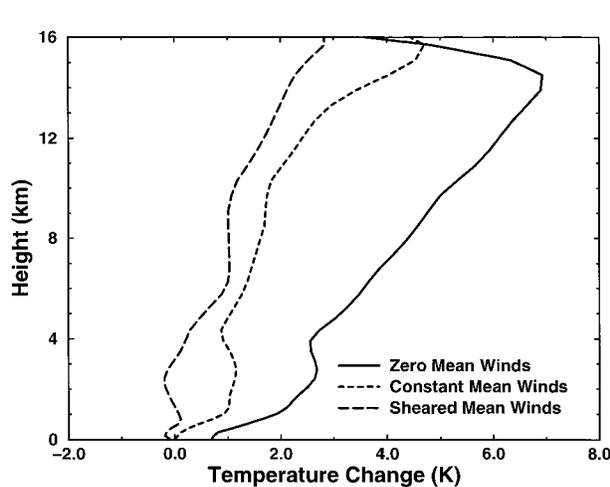

FIG. 15. Temperature difference against height between 2D and 3D experiments for the zero (control), constant, and sheared wind experiments.
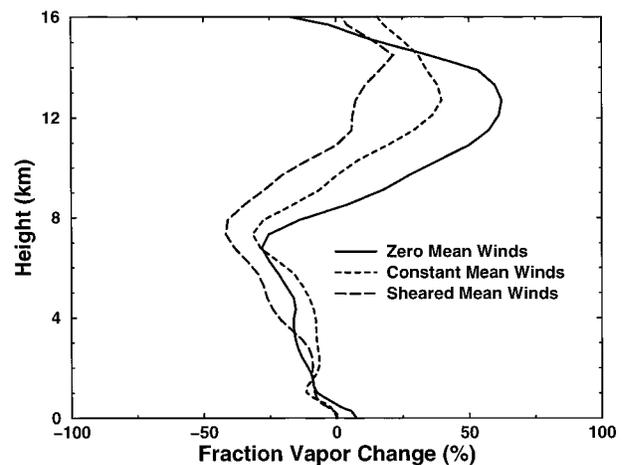

FIG. 16. Fractional water vapor change against height between 2D and 3D experiments for the zero (control), constant, and sheared wind experiments. Fractional change calculated as $(r^{2D} - r^{3D})/r^{2D}$, where r represents the water vapor mass mixing ratio.

TABLE 4. Final thermodynamic states for 120-km 2D experiments.

Experiment	Mean temperature (K)	Total water vapor (kg m^{-2})
Zero mean winds	254.4	41.3
Constant 4 m s^{-1} mean winds	257.3	48.0
Sheared mean winds	258.6	59.8

until the next convective event occurs. Thus, although 2D geometry can artificially increase surface perturbation winds, using an undersized 2D domain artificially restricts them again.

Above the boundary layer, the restriction of mesoscale organization in the small 2D domains produces very similar vapor profiles, although there is a considerable amount of vertical variation since many fewer clouds occur during the 5-day averaging period in the small 2D domain. The difference between 2D and 3D does not usually exceed the standard deviation of the small 2D run, with the exception of the upper troposphere. The temperature profiles are also very similar with the difference remaining less than 1 K below about 10 km.

6. Discussion

Figure 19 shows a schematic of convection in a large domain of say O(100 km) by O(1000 km) in reality, and in 2D and 3D simulations. Without strong large-scale organization factors, cumulus clouds can assume random distributions, but in particular if deep convection is present, cumulus cloud fields are often observed to cluster (as in Fig. 19a) on a variety of spatial scales (Nair et al. 1998). This can be due to a variety of processes such as propagation via downdraft outflow, the enhanced water vapor signature of previous clouds, or via cloud–radiation interactions (Tompkins and Craig 1998a), for example.

It is also possible, that other organizational effects, such as a sea surface temperature (SST) gradient or large vertical wind shear, can strongly organize the convection in one horizontal direction (illustrated in 19b) rendering a quasi 2D large-scale flow. Since this "external" organization will likely override the spontaneous organization that occurred in the 2D long-domain simulations in this paper, it is likely that 2D simulations can reasonably be used, provided that the domain is sufficiently long to contain the wavelength of the organization (e.g., the subsidence region associated with a squall line), and provided that mean surface winds are greater than typical convection downdraft outflow speeds.

Two-dimensional simulations (Fig. 19c) always force convection to be in the state with the largest possible cloud cluster separation, however, even in the absence of other organizational effects, and lead to self-organization of convection via water vapor feedback. It is
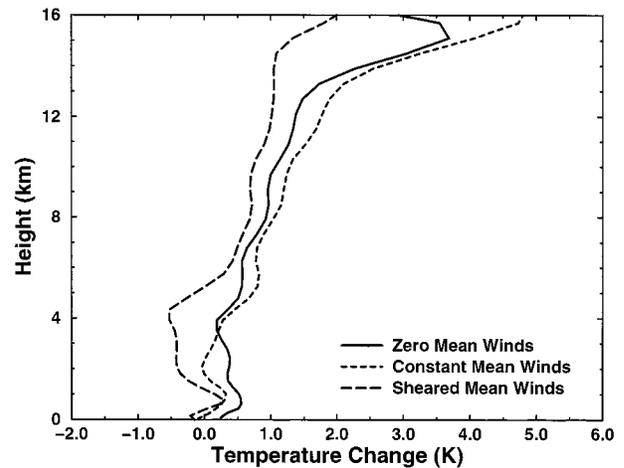

FIG. 17. Temperature difference against height between the 3D and short domain 120-km 2D experiments for the zero (control), constant, and sheared wind experiments.

likely that, if the same spontaneous water vapor organization of convection occurred in a large domain 3D experiment at all, it would occur on shorter horizontal spatial scales. Therefore in these situations, where strong 2D organizational effects are absent, and convection is randomly distributed or clustered, a 3D model should be used. Indeed, it has been shown that a 3D model is anyway necessary if mean surface winds are low. That said, if the forcing for convection is imposed and noninteractive, highly intermittent convective activity is not a problem, and only estimates of general bulk atmospheric quantities are required that are not sensitive to the fine detail of surface flux and boundary layer processes, then computationally cheap, limited domain 2D experiments are possible.
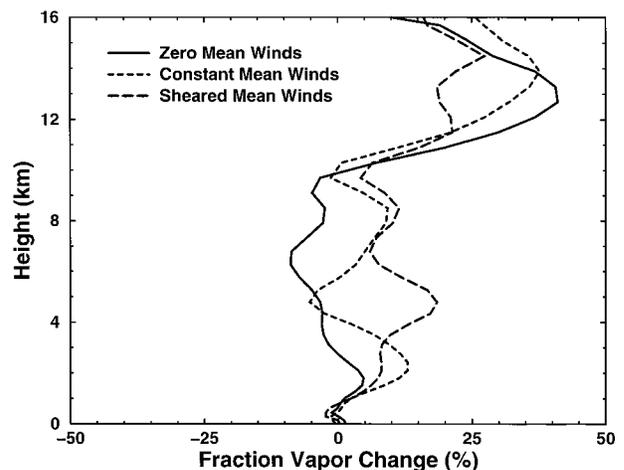
Finally, it should be noted that small 3D domains that

FIG. 18. Fractional water vapor change against height between the 3D and short domain 120-km 2D experiments for the zero (control), constant, and sheared wind experiments. Fractional change calculated as in Fig. 16.

can support only a few concurrent convective events (Fig. 19d) impose a greater level of regularity on the cloud field, and reduce root mean intercloud separation (leading to moister equilibrium atmospheres) since any processes leading to clustering can be expressed only in association with convective intermittency, and are therefore probably suppressed. This simply implies that the minimum 3D domain size is one that is large enough to contain the subsidence associated with the system of convection on the largest scale one is interested in studying. This will be investigated further in a companion paper to this one that simulates Walker cell-like circulations in 3D domains of $O(100$ km$)$ by $O(1000$ km$)$.

7. Conclusions

Even 2D convective systems such as squall lines contain 3D cloud-scale motions, and so it is impossible to expect 2D and 3D simulations to render identical results. However, given the large investment that has been previously made in 2D CRM simulations, it is important to appreciate if significant differences develop in the mean thermodynamic states over time, due solely to the geometry of the simulations. To examine this, a number of long-term 2D and 3D CRM experiments were made and compared. Cloud–radiation interactions were removed by applying a fixed constant forcing for convection. Thus, the experiments were rendered more easy to understand by removing this feedback with radiation, but it should be noted that the differences and trends observed could be much larger (or indeed smaller) if an interactive radiation scheme were to be used.

Preliminary investigations proved the conjecture of Tompkins and Craig (1998a) that the intermittency of convection is independent of dimensionality. Provided that convective quantities such as updraft strength and horizontal scale remain largely unchanged, the intuitive conception that convection will occur more frequently when a specific number of grid points are arranged in a ''long'' 2D domain, instead of its 3D equivalent, is false.

The main control run, which compared a 60 km × 60 km 3D domain with an 1800-km 2D domain containing the same number of grid points revealed major differences in final state statistics. Although the radiative forcing for convection constrains net convective and total mass fluxes and cloud characteristics to be similar, and also forces the total surface fluxes to be the same in each case, the 2D run had a warmer and moister boundary layer leading to the adoption of a warmer moist-adiabatic temperature profile. In contrast, the majority of the troposphere above the boundary layer was drier in 2D. Two mechanisms were suggested to explain these differences:

- The different geometries of two and three dimensions lead to higher mean surface perturbation winds in 2D
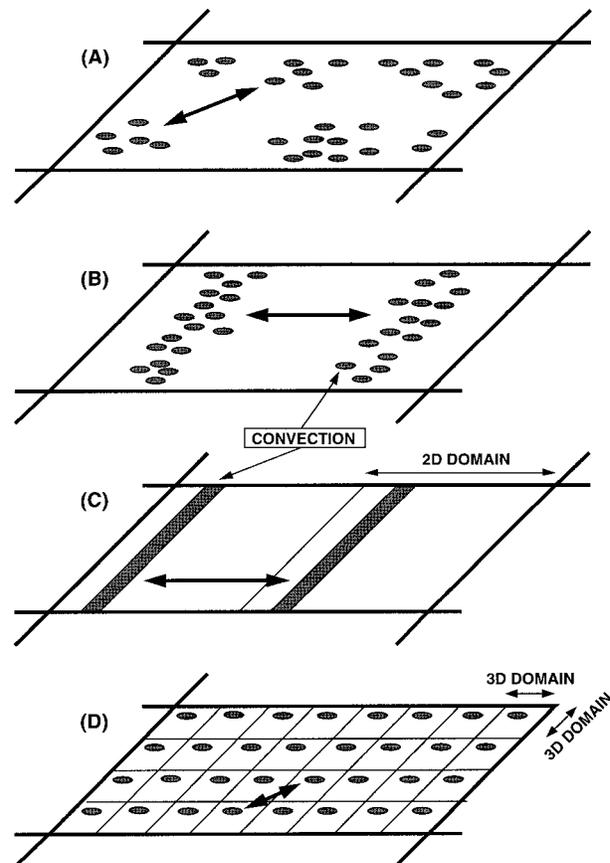

FIG. 19. Schematic showing organization that occurs in 2D and 3D simulations, and in reality, for some arbitrarily large domain. The double-headed arrow represents the typical intercloud or intercloud cluster spacing. In the absence of strong external organizational factors, clouds will be randomly spaced or exhibit clustering (A). However, strong horizontal organization factors such as SST gradients or strong mean wind shear can organize convection into quasi 2D structures (B), which will have a larger ''intercluster spacing'' than randomly distributed clouds. A 2D simulation (C) imposes the largest possible intercloud spacing even in cases where no external organization exists. Using the same number of grid points as in a 3D domain (D) imposes regularity on the fields and reduces the intercloud spacing to a minimum. See text for discussion. For simplicity the simulation domains in (C) and (D) are assumed to be of the order of magnitude in size to continuously contain one convective event.

resulting from convective downdrafts. This gives a warmer and moister boundary layer in equilibrium.
- In the 2D experiments mesoscale organization of convection occurs. Convection is encouraged to reoccur in regions that have already experienced convection and are therefore more humid.

In further experiments it was found that applying a constant mean wind of 4 m s^{-1} was already enough to negate most of the differences in thermodynamic states due to the surface flux mechanism described above, since convective downdrafts then act to both reduce and enhance local winds and thus do not change mean surface fluxes. However, the convection remained orga-

nized in this case, and also when a vertical wind shear was applied, and thus differences in the vapor profiles remained. Note that no Coriolis force was applied in these experiments, which were assumed to take place over equatorial ocean. The application of the Coriolis force could have also reduced the magnitude of the 2D perturbation velocities by restricting the downdraft outflow radius.

Using a small 120-km 2D domain artificially constrains surface perturbation velocities, and also prevents the large-scale organization of convection, and therefore gave similar results to the 3D runs. However, it is strongly suspected that if an interactive radiation scheme provided the forcing for convection it is highly unlikely that limited 2D domain modeling would be acceptable, due to the extreme intermittency of convection and the nonlinearity of radiation.

The results reported here do not contradict earlier 2D–3D investigations. The differences in mean thermodynamic states were revealed only after several days, and would not have been apparent in short-term simulations. Additionally, the comparisons of Grabowski et al. (1998) used an imposed mean vertical wind shear with a substantial surface wind velocity, and many fewer grid points in the 2D experiments. The investigations here have shown that the mean surface wind speed renders the boundary layer characteristics identical, giving similar temperature profiles, while the restricted 2D domain prevents organization of convection, and forces similar profiles for the water vapor.

In conclusion, it would appear that for modeling convection that is highly two-dimensionally organized, such as squall lines or Walker-type circulations over strong SST gradients, and for which a mean surface wind exists that exceeds typical downdraft outflow velocities, it is possible that a 2D model can give reasonable results. However, for random distributed or clustered convection, and especially in low wind environments, it is highly preferable to use a 3D cloud model.

REFERENCES

Anthes, R. A., 1977: A cumulus parameterization scheme utilising a one-dimensional cloud model. *Mon. Wea. Rev.,* **105,** 270–286.

Bretherton, C. S., and P. K. Smolarkiewicz, 1989: Gravity waves, compensating subsidence and detrainment around cumulus clouds. *J. Atmos. Sci.,* **46,** 740–759.

Brown, P. R. A., and H. A. Swann, 1997: Evaluation of key micro- physical parameters in three dimensionsal cloud model simu- lations using aircraft and multiparameter radar data. *Quart. J. Roy. Meteor. Soc.,* **123,** 2245–2275.

Brown, R. G., and C. Zhang, 1997: Variability of midtropospheric moisture and its effect on cloud-top height distribution during TOGA COARE. *J. Atmos. Sci.,* **54,** 2760–2774.

Browning, K. A., and F. H. Ludham, 1962: Airflow in convective storms. *Quart. J. Roy. Meteor. Soc.,* **88,** 117–135.

Cheng, M.-D., 1989: Effects of downdraughts and mesoscale con- vective organization on the heat and moisture budgets of tropical cloud clusters. Part II: Effects of convective-scale downdrafts. *J. Atmos. Sci.,* **46,** 1540–1564.

Dharssi, I., R. Kershaw, and W.-K. Tao, 1997: Sensitivity of a sim- ulated tropical squall line to long-wave radiation. *Quart. J. Roy. Meteor. Soc.,* **123,** 187–206.

Emanuel, K. A., 1991: A scheme for representing cumulus convection in large-scale models. *J. Atmos. Sci.,* **48,** 2313–2335.

——, 1994: *Atmospheric Convection.* Oxford University Press, 580 pp.

Grabowski, W. W., M. W. Moncrieff, and J. T. Kiehl, 1996a: Long- term behaviour of precipitating tropical cloud systems: A nu- merical study. *Quart. J. Roy. Meteor. Soc.,* **122,** 1019–1042.

——, X. Wu, and M. W. Moncrieff, 1996b: Cloud-resolving modeling of tropical cloud systems during Phase III of GATE. Part I: Two- dimensional experiments. *J. Atmos. Sci.,* **53,** 3684–3709.

——, ——, ——, and W. D. Hall, 1998: Cloud-resolving modeling of cloud systems during Phase III of GATE. Part II: Effects of resolution and the third spacial dimension. *J. Atmos. Sci.,* **55,** 3264–3282.

Guichard, F., J.-P. Lafore, and J.-L. Redelsperger, 1997: Thermody- namical impact and internal structure of a tropical convective cloud system. *Quart. J. Roy. Meteor. Soc.,* **123,** 2297–2324.

Held, I. M., R. S. Hemler, and V. Ramaswamy, 1993: Radiative– convective equilibrium with explicit two-dimensional moist con- vection. *J. Atmos. Sci.,* **50,** 3909–3927.

Islam, S., R. L. Bras, and K. A. Emanuel, 1993: Predictability of mesoscale rainfall in the Tropics. *J. Appl. Meteor.,* **32,** 297–310.

Lau, K.-M., C. H. Sui, and W. K. Tao, 1993: A preliminary study of the tropical water cycle and its sensitivity to surface warming. *Bull. Amer. Meteor. Soc.,* **74,** 1313–1321.

LeMone, M. A., and E. J. Zipser, 1980: Cumulonimbus vertical ve- locity events in GATE. Part I: Diameter, intensity and mass flux. *J. Atmos. Sci.,* **37,** 2444–2457.

Leonard, B. P., 1991: The ULTIMATE conservative difference scheme applied to unsteady one-dimensional advection. *Comput. Methods Appl. Mech. Eng.,* **19,** 17–74.

Mapes, B. E., and P. Zuidema, 1996: Radiative–dynamical conse- quences of dry tongues in the tropical troposphere. *J. Atmos. Sci.,* **53,** 620–638.

Michaud, L. M., 1998: Entrainment and detrainment required to ex- plain updraft properties and work dissipation. *Tellus,* **50A,** 283– 301.

Nair, U. S., R. C. Weger, K. S. Kuo, and R. M. Welch, 1998: Clus- tering, randomness, and regularity in cloud fields 5. The nature of regular cumulus clouds fields. *J. Geophys. Res.,* **103,** 11 363– 11 380.

Raymond, D. J., 1995: Regulation of moist convection over the west Pacific warm pool. *J. Atmos. Sci.,* **52,** 3945–3959.

Robe, F. R., and K. A. Emanuel, 1996: Dependence of tropical con- vection on radiative forcing. *J. Atmos. Sci.,* **53,** 3265–3275.

Schlesinger, R. E., 1973: A numerical model of deep moist convec- tion. Part 1: Comparative experiments for variable ambient mois- ture and wind shear. *J. Atmos. Sci.,* **30,** 835–856.

——, 1978: A three dimensional numerical model of an isolated thunderstorm. Part 1: Comparative experiments for variable am- bient wind shear. *J. Atmos. Sci.,* **35,** 690–713.

Shutts, G. J., and M. E. B. Gray, 1994: A numerical modelling study of the geostrophic adjustment following deep convection. *Quart. J. Roy. Meteor. Soc.,* **120,** 1145–1178.

Sui, C. H., K. M. Lau, W. K. Tao, and J. Simpson, 1994: The tropical

water and energy cycles in a cumulus ensemble model. Part I: Equilibrium climate. *J. Atmos. Sci.,* **51,** 711–728.

Tao, W. K., and S.-T. Soong, 1986: A study of the response of deep tropical convection to mesoscale processes: Three-dimensional numerical experiments. *J. Atmos. Sci.,* **43,** 2653–2676.

——, J. Simpson, and S.-T. Soong, 1987: Statistical properties of a cloud ensemble: A numerical study. *J. Atmos. Sci.,* **44,** 3175–3187.

Tompkins, A. M., and G. C. Craig, 1998a: Radiative–convective equilibrium in a three-dimensional cloud ensemble model. *Quart. J. Roy. Meteor. Soc.,* **124,** 2073–2097.

——, and ——, 1998b: Timescales of adjustment to radiative–convective equilibrium in the tropical atmosphere. *Quart. J. Roy. Meteor. Soc.,* **124,** 2693–2713.

——, and ——, 1999: Sensitivity of tropical convection to sea surface temperature in the absence of large-scale flow. *J. Climate,* **12,** 462–476.

——, and K. A. Emanuel, 2000: The vertical resolution sensitivity of simulated equilibrium temperature and water vapour profiles. *Quart. J. Roy. Meteor. Soc.,* in press.

Wyant, M. C., C. S. Bretherton, H. A. Rand, and D. E. Stevens, 1997: Numerical simulations and a conceptual model of the stratocumulus to trade cumulus transition. *J. Atmos. Sci.,* **54,** 168–192.

Xu, K.-M., and S. K. Krueger, 1991: Evaluation of cloudiness parameterizations using a cumulus ensemble model. *J. Atmos. Sci.,* **48,** 342–367.

——, and A. Arakawa, 1992: Semiprognostic tests of the Arakawa–Schubert cumulus parameterization using simulated data. *J. Atmos. Sci.,* **49,** 2421–2436.